Electronic Supporting Information for

Intermediates and Mechanism in Iron-Catalyzed C-H Methylation with Trimethylaluminum

Shilpa Bhatia,‡ Joshua C. DeMuth,‡ Michael L. Neidig*

Department of Chemistry, University of Rochester, Rochester, New York 14627, USA

Table of Contents

1. Experimental

1.1 General Considerations. Unless noted otherwise, all starting materials were prepared using literature protocols.[1, 2] Reagents were purchased commercially and used without additional purification. Anhydrous solvents were further dried through activated-alumina filtration and stored on 4 Å molecular sieves under an inert nitrogen atmosphere. An enriched iron source of $^{57}Fe(acac)_3$ was used for Mössbauer sample preparation and was synthesized using a previously published procedure with $^{57}Fe_2O_3$ (95%+ enriched) purchased from Isoflex.[3] All moisture and air-sensitive experiments were conducted in an MBraun inert-atmosphere N_2 glovebox equipped with a liquid nitrogen transfer line permitting rapid freeze-trapping of reaction samples for spectroscopic analysis. Additional experimental details are outlined in the electronic supporting information.

1.2 Experimental Methods

1.2.1 Mössbauer Spectroscopy. Freeze-trapped samples were prepared using enriched $^{57}Fe(acac)_3$ under inert nitrogen atmosphere in a glovebox equipped with a liquid nitrogen transfer port to allow rapid freezing at 77 K. Samples were loaded into Delrin cups and subsequently freeze-trapped in liquid nitrogen. Low-temperature ^{57}Fe Mössbauer spectroscopic analysis was performed using a Janis SVT-400T N2 cryostat for analysis at 80 K. Isomer shift values were calibrated against an α-Fe standard at 298 K. Fitting of the Mössbauer data was performed using WMoss (See Co.) software. The corresponding errors in the fit analyses include the following: $\delta \pm 0.02$ mm/s, $|\Delta E_Q| \pm 3$ %, multicomponent fit quantitation error of ± 3 %. Only zero-field Mossbauer measurements were collected, hence all quadrupole splitting parameters are reported as absolute values. Catalytic solution Mössbauer samples were prepared following the literature protocol for the catalysis and rapid freeze-trapping at specified timepoints.[1, 2]

1.2.2 Electron Paramagnetic Resonance Spectroscopy. Catalytic solution EPR samples were prepared following the literature protocol for the catalysis and rapid freeze-trapping at specified timepoints.[1, 2] In situ stoichiometric samples were prepared as described in the text and freeze-trapped at the specified timepoints. Spin integrated EPR samples were prepared in high-precision 4 mm OD Suprasil quartz EPR tubes from Wilmad Labglass, which allowed direct evaluation of signal intensities between samples. Samples were spin-integrated against an external standard of $CuSO_4 \bullet 5H_2O$ under non-saturating conditions. X-band EPR measurements were collected on a Bruker EMXplus spectrometer equipped with a 4119HS cavity and an Oxford ESR-900 helium flow cryostat.

1.2.3 ^{1}H, ^{2}H, ^{31}P NMR Spectroscopy. All NMR spectroscopic measurements were performed on a Bruker Avance 400 MHz NMR spectrometer at ambient temperature. Quantitative ^{1}H NMR analyses were performed with 1,3,5-trimethoxybenzene as an internal standard. Chemical shifts (δ) are reported in parts per million (ppm), and calibrated using the internal standard (1,3,5-trimethoxybenzene, 6.08 ppm) or residual solvent signals for ^{1}H NMR, the presence of naturally abundant deuterated solvent signals (THF-d_8 1.73/3.58 ppm) for ^{2}H NMR, or non-ligated bisphosphine for ^{31}P NMR.

1.3 Stoichiometric reaction of 4m with DCB. A 20 mL scintillation vial was charged with $^{57}Fe(acac)_3$ (0.0106 g, 0.03 mmol), $Fe(acac)_3$ (0.0071 g, 0.02 mmol), **sub-AQ** (0.0131 g, 0.05 mmol), and THF (3.4 mL) and stirred for 10 minutes at room temperature followed by stirring for 10 minutes at 35 °C. In a separate 20 mL scintillation vial, a solution of MeMgBr (98 μL, 1.025 M in hexane, 0.1 mmol) in THF (3.3 mL) was prepared and added to the above $Fe(acac)_3$/**sub-AQ** solution dropwise over 10 mins at 35 °C and stirred for another 10 mins. In another 20 mL scintillation vial, a solution of dppen (0.0198g, 0.05mmol) with MeMgBr (98 μL, 1.025 M in hexane, 0.1 mmol) in THF (3.3 mL) was prepared and subsequently added to the above solution dropwise over 10 mins at 35 °C. The resulting dark solution was stirred for 30 seconds and 3 ml of the solution was transferred to another 20 mL scintillation vial pre-heated at 35 °C for control samples. 1 ml from the control vial was freeze-trapped for ^{57}Fe Mössbauer analysis followed by addition of DCB (200 μL) to the remaining 7 mL solution in the original vial. 1 mL aliquots of the resulting solution were freeze-trapped at various timepoints for ^{57}Fe Mössbauer analysis. A duplicate experiment was performed for NMR analysis where samples were prepared by chemically quenching 1 mL aliquots of solution with water for analysis of product formation.

1.4 Preparation of $Fe(dppen)_2(Me)_2$. $^{57}Fe(acac)_3$ (0.071 g, 0.02 mmol), $Fe(acac)_3$ (0.0246 g, 0.07 mmol), dppen (0.0715 g, 0.18 mmol), and THF (15 mL) was added to a 20 mL scintillation vial and stirred for 30 minutes at room temperature. In a separate 20 mL scintillation vial, a solution of $AlMe_3$ (675 μL, 2 M in hexane) in THF (15 mL) was prepared. The $Fe(acac)_3$/dppen solution was then transferred to a 100 mL round bottom flask and pre-heated to 55 °C on an aluminum pie-block for 20 minutes. Next, the solution of $AlMe_3$ was added dropwise (750 μL/min, 20 min) to the solution of iron and bisphosphine at 55 °C. After the addition, the flask was transferred to an oil recirculating bath cooled aluminum pie-block at 0 °C and concentrated to an overall volume of 9 mL. The concentrated solution was then split equally between three 20 mL scintillation vials. To each scintillation vial, 4.5 mL of chilled hexane (0 °C) was added while stirring. After stirring for two minutes, the solution was allowed to settle for five minutes at 0 °C. Each vial of solution was then filtered through a 1 cm Celite pad into clean 20 mL scintillation vials. The vials were then stored in a -30 °C freezer. Red-orange crystals were observed in each vial within 12-24 h.

2. Supplementary Spectroscopic Data

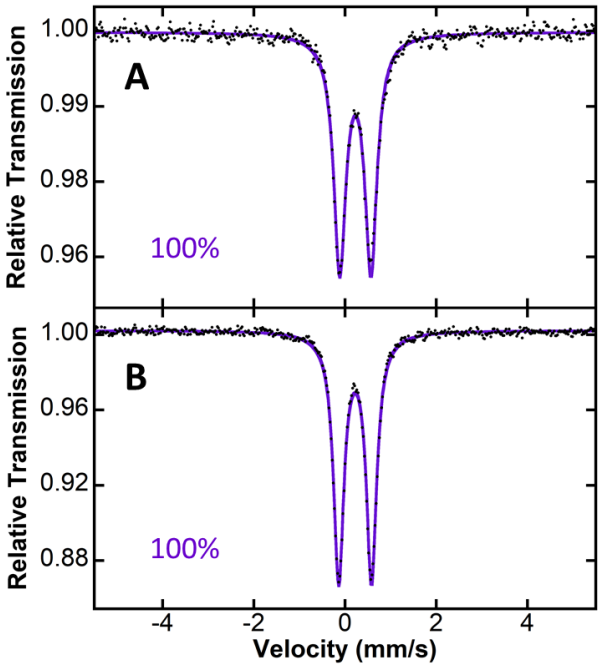

Figure S1. 80 K ^{57}Fe Mössbauer spectra of crystalline Fe(dppen)$_2$(Me)$_2$ (**5m**) (A) crushed into fine powder and (B) redissolved in THF. Data (black dots) and fit components are shown. Purple component for the solid spectrum has parameters δ = 0.22 mm/s and $|\Delta E_Q|$ = 0.69 mm/s and for the solution spectrum has parameters δ = 0.22 mm/s and $|\Delta E_Q|$ = 0.72 mm/s.

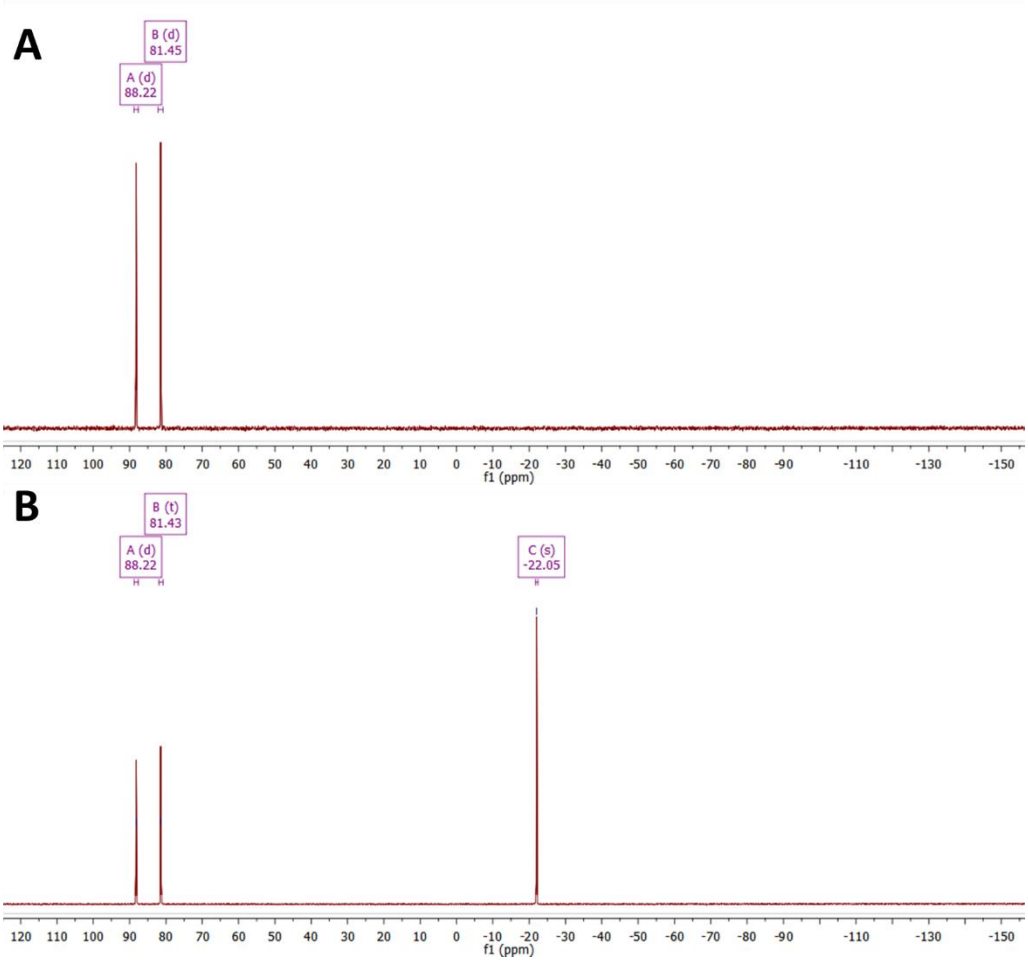

Figure S2. ^{31}P NMR spectra of (A) a solution of Fe(Me)$_2$(dppen)$_2$ (**5m**) crystals dissolved in THF-d_8 and (B) a similar solution spiked with non-ligated dppen (-22 ppm).

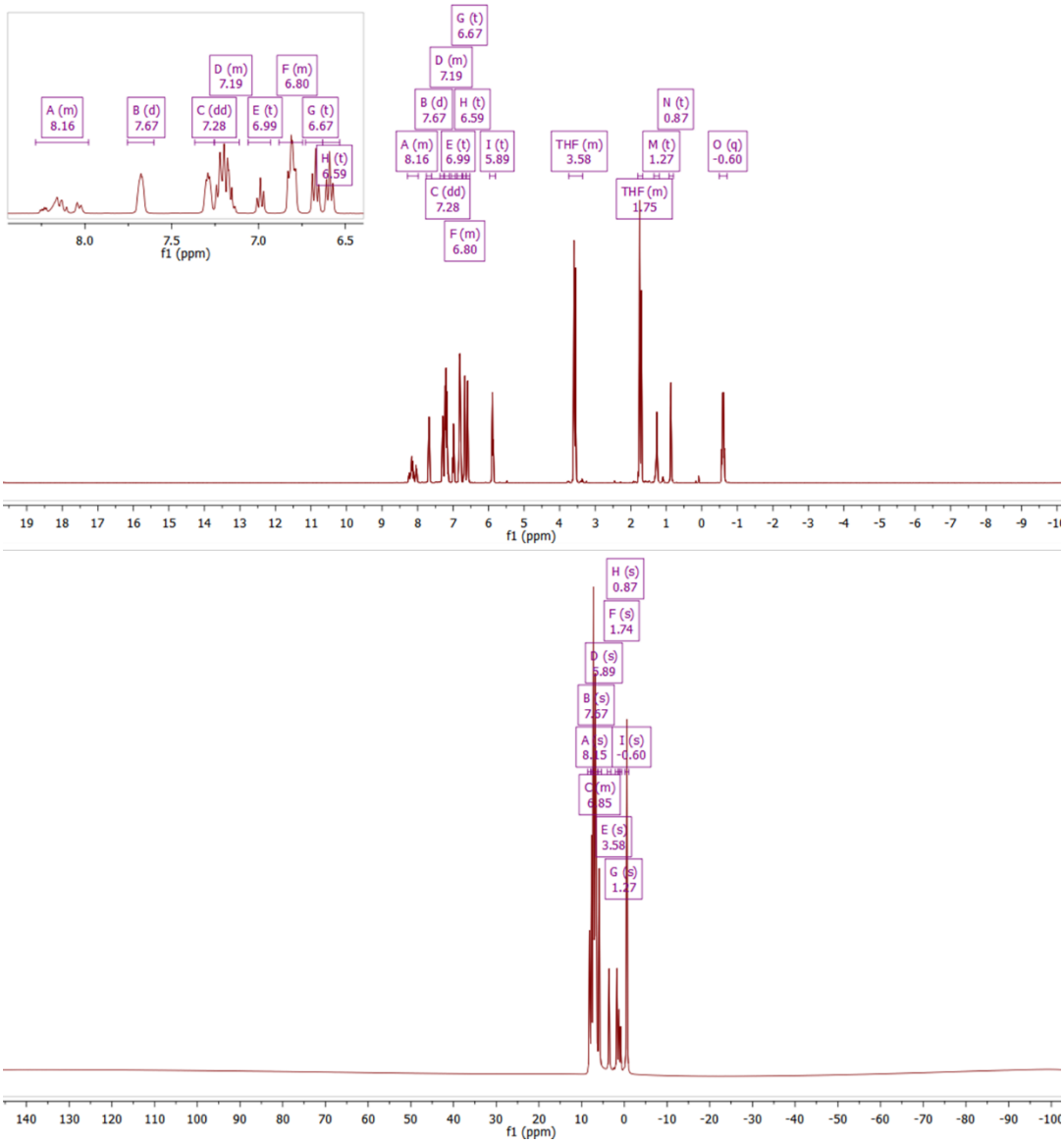

Figure S3. Paramagnetic ^{1}H NMR spectrum (top) and diamagnetic ^{1}H NMR spectrum (bottom) of crystalline $Fe(Me)_2(dppen)_2$ (**5m**) dissolved in THF-d_8. The absence of signals beyond the diamagnetic range are consistent with the assignment of this species as diamagnetic.

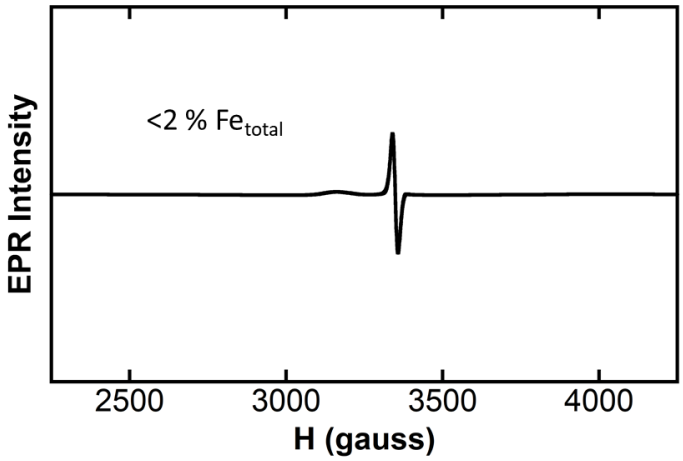

Figure S4. 10 K EPR analysis 10 minutes after the dropwise addition of $AlMe_3$ (2.0 equiv) to a solution of **sub-AQ** (1.0 equiv), $Fe(acac)_3$ (1.0 mol %), and dppen (1.1 mol %) in THF at RT. The g-value corresponds to an S = ½ species quantified at less than 2 % of the total iron in solution.

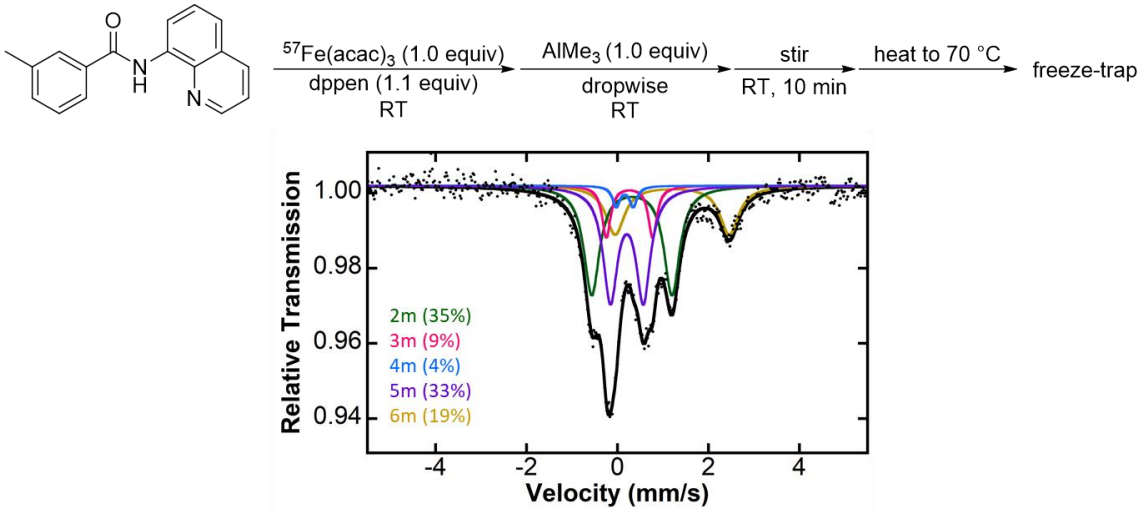

Figure S5. Freeze-quenched 80 K ^{57}Fe Mössbauer spectrum following the reaction of a solution of sub-AQ (1.0 equiv), $Fe(acac)_3$, and dppen (1.1 equiv) with $AlMe_3$ (1.0 equiv) at RT for 10 min then heated to 70 °C for 5 min. The green species has parameters δ = 0.32 mm/s and $|\Delta E_Q|$ = 1.76 mm/s consistent with **2m**. The pink species has parameters δ = 0.27 mm/s and $|\Delta E_Q|$ = 1.02 mm/s consistent with **3m**. The light blue has parameters δ = 0.16 mm/s and $|\Delta E_Q|$ = 0.37 mm/s consistent with **4m**. The purple species has parameters δ = 0.21 mm/s and $|\Delta E_Q|$ = 0.73 mm/s consistent with $Fe(dppen)_2(Me)_2$ (**5m**). The yellow species (**6m**) has parameters δ = 1.21 mm/s and $|\Delta E_Q|$ = 2.51 mm/s consistent with a high-spin iron(II) complex, an assignment further confirmed by its formation by reduction of $Fe(acac)_3$ with $AlMe_3$ (Figure S10).

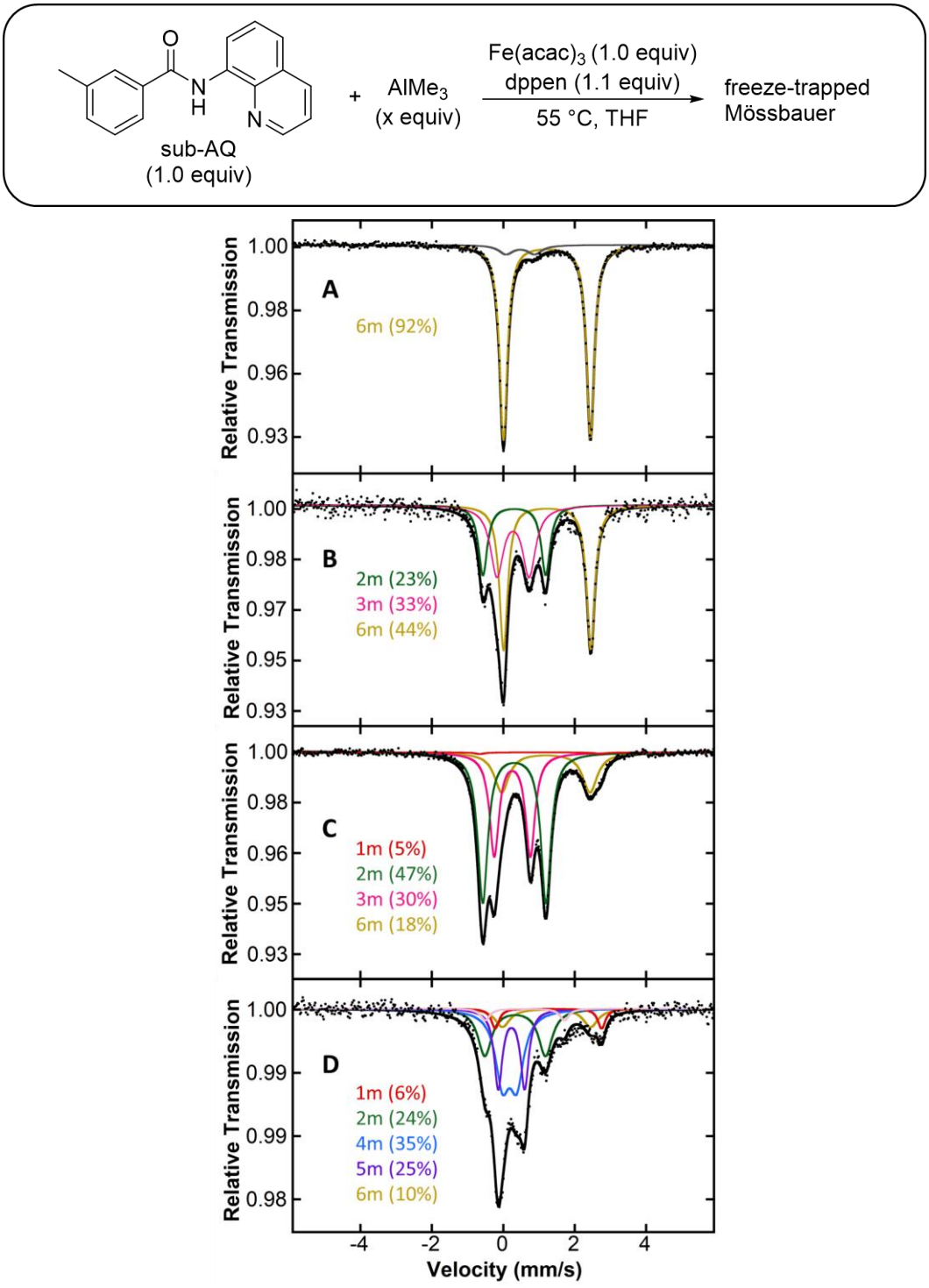

Figure S6. Freeze-quenched 80 K ^{57}Fe Mössbauer spectrum following the reaction of a solution of sub-AQ (1.0 equiv), $Fe(acac)_3$ (1.0 equiv), and dppen (1.1 equiv) with (A) 0.33 equiv (B) 0.67 equiv, (C) 1.0 equiv, and (D) 1.33 equiv $AlMe_3$ at 55 °C.

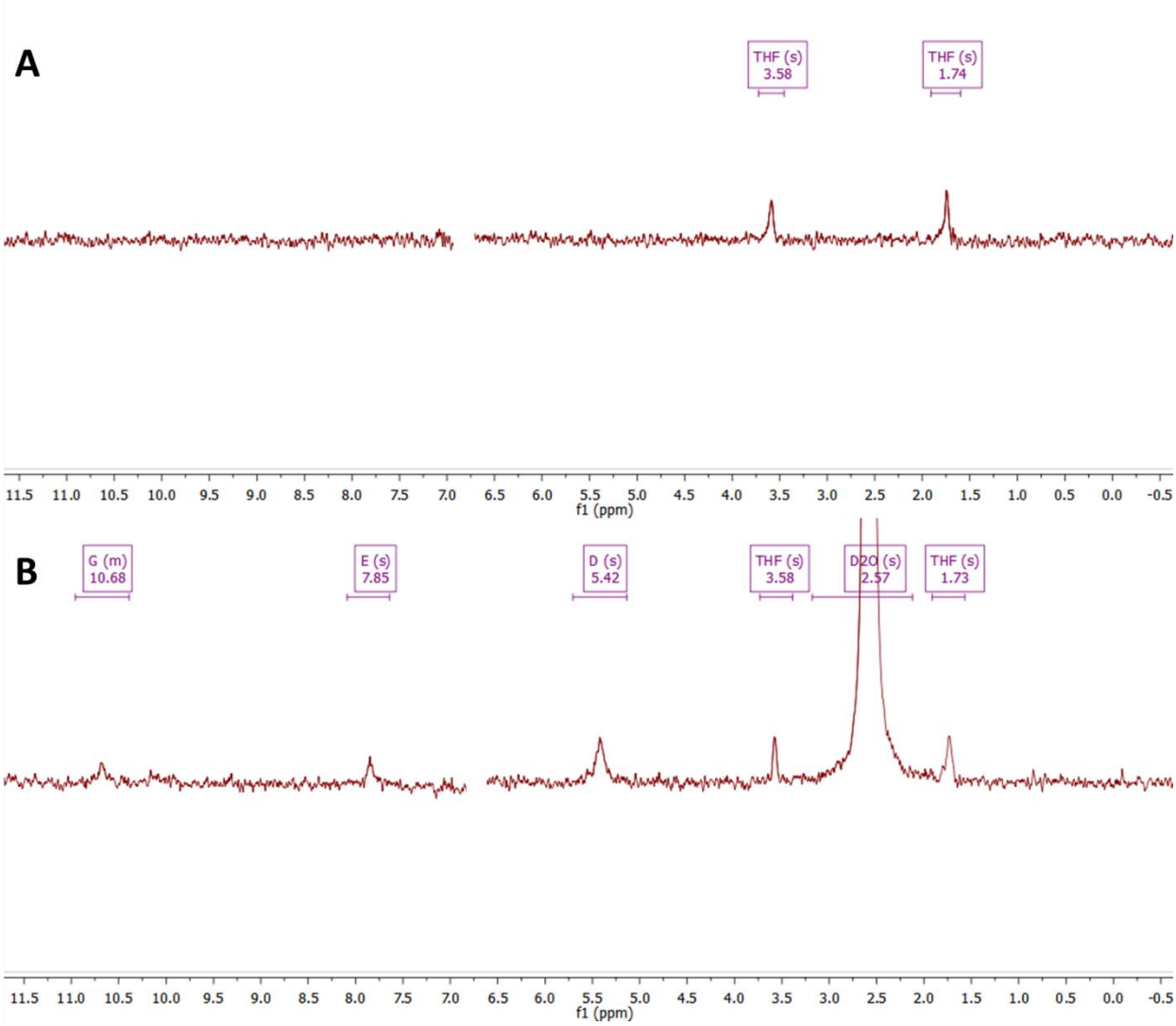

Figure S7. The ^{2}H NMR spectrum of (A) in situ generated **2m** (47 % total iron) and **3m** (30 %) with minor amounts of **1m** and a high-spin iron(II) **6m** and (B) the ^{2}H NMR spectrum following a chemical quench of that solution with excess deuterium oxide. The presence of signal in the aromatic region (7.85 ppm) is consistent with aromatic deuterium incorporation resulting from the quenching of a cyclometalated iron species. The signals at 3.58 ppm and 1.73 ppm are from the presence of THF-d_8 in natural abundance. The region containing 6.70-6.80 ppm contains an instrument artifact in ^{2}H NMR and cannot be used. The signal at 10.68 ppm is consistent with deuterium incorporation at the amide nitrogen, and the signal at 5.42 ppm is consistent with deuterium incorporation of acetylacetonate ligand.

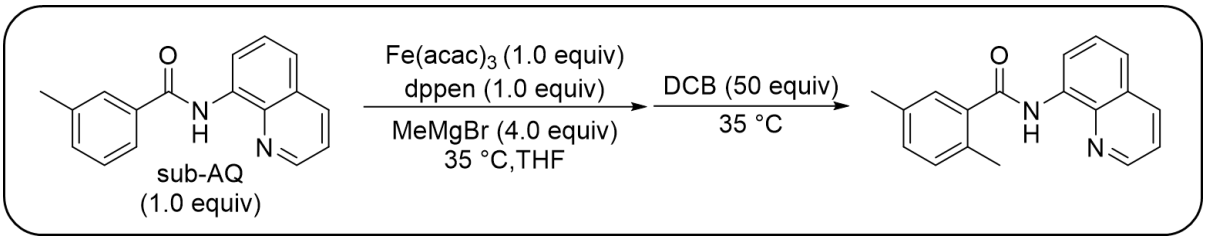

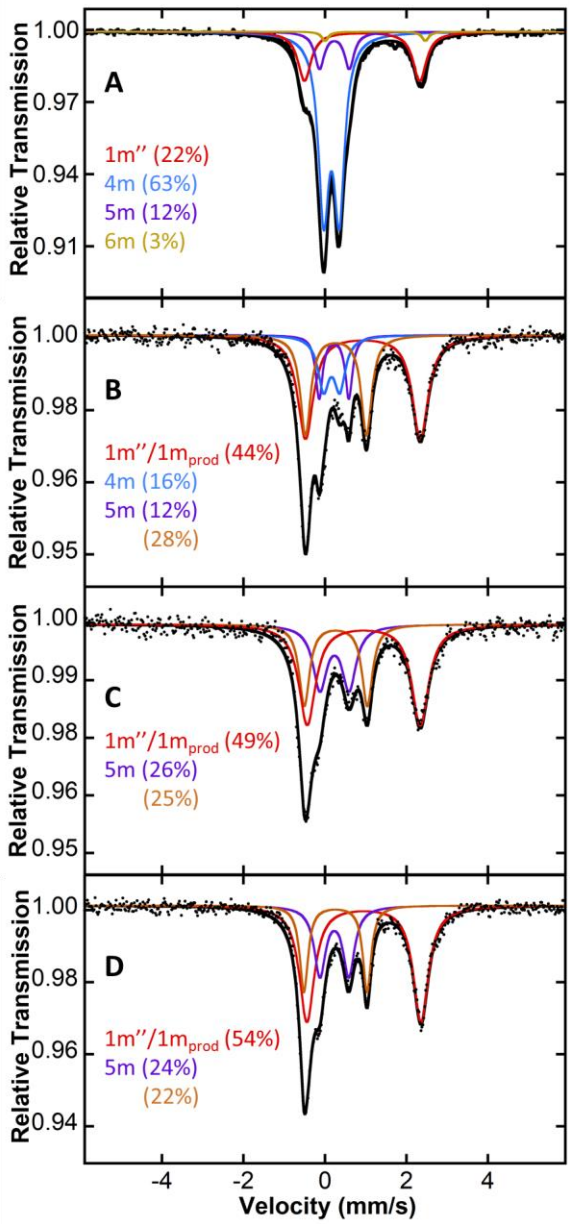

Figure S8. 80 K ^{57}Fe Mössbauer spectrum of (A) a freeze-trapped solution following the reaction of **sub-AQ** (1.0 equiv), $Fe(acac)_3$ (1.0 equiv), and dppen (1.0 equiv) with MeMgBr (4.0 equiv) at 35 °C, and the subsequent reaction with excess DCB (50 equiv) at 35 °C for (B) 30 s, (C) 1 min, and (D) 10 min. Data (black dots) and fit components are shown. Blue component **4m** has parameters δ = 0.16 mm/s and $|\Delta E_Q|$ = 0.39 mm/s. The orange component has parameters δ = 0.26 mm/s and $|\Delta E_Q|$ = 1.51 mm/s. Note that the parameters of the red component are consistent with those of **1m/1m'**, however a **1m''** notation is used as an analogue with a bromide ligand cannot be excluded. Similarly, a product bound analogue of this species (**1m$_{prod}$**) bearing a bromide ligand could also form upon reaction of **4m** with oxidant.

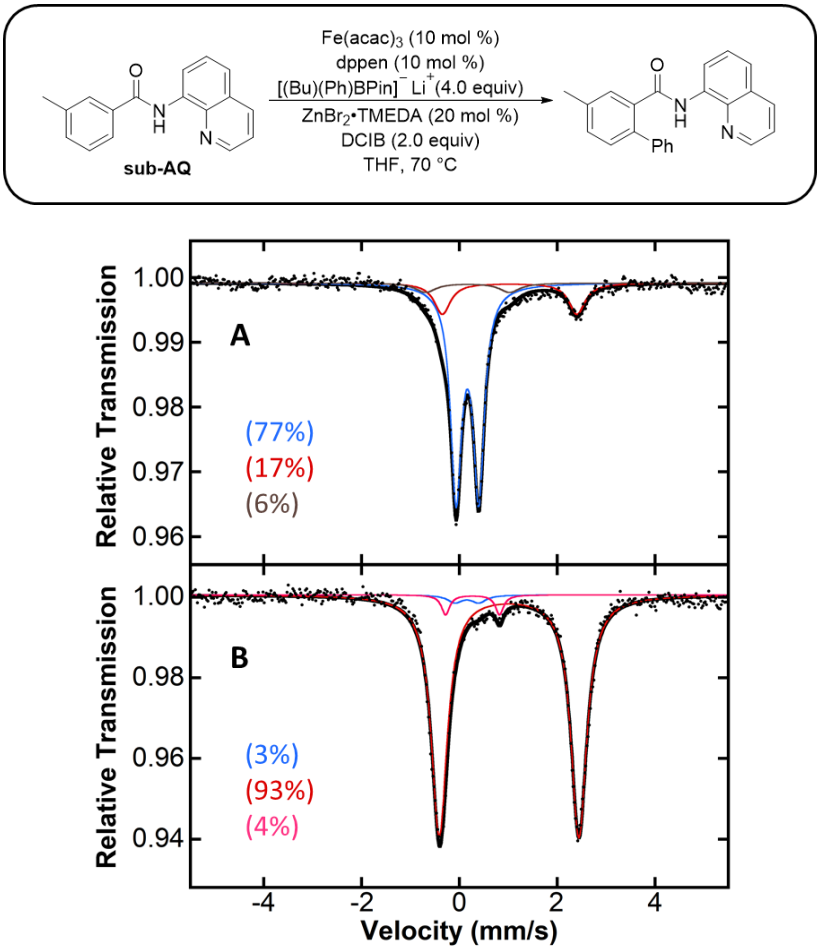

Figure S9. 80 K ^{57}Fe Mössbauer spectrum of the iron-catalyzed arylation of **sub-AQ** with phenylboronate reagent freeze-quenched following (A) one hour and (B) four hours of reaction. Data (black dots) and fit components are shown. The corresponding 5 K EPR spectra at both timepoints revealed that the major species are EPR silent. The individual component Mössbauer parameters are the following: blue component, δ = 0.16 mm/s and $|\Delta E_Q|$ = 0.47 mm/s, red component, δ = 1.02 mm/s and $|\Delta E_Q|$ = 2.80 mm/s, dark brown component has parameters δ = 0.17 mm/s and $|\Delta E_Q|$ = 1.72 mm/s, and pink component, δ = 0.27 mm/s and $|\Delta E_Q|$ = 1.10 mm/s. Note that the parameters of the blue component are similar to those of the low-spin cyclometalated species **4m**, while the parameters of the red component are consistent with those of a high-spin iron(II) species.

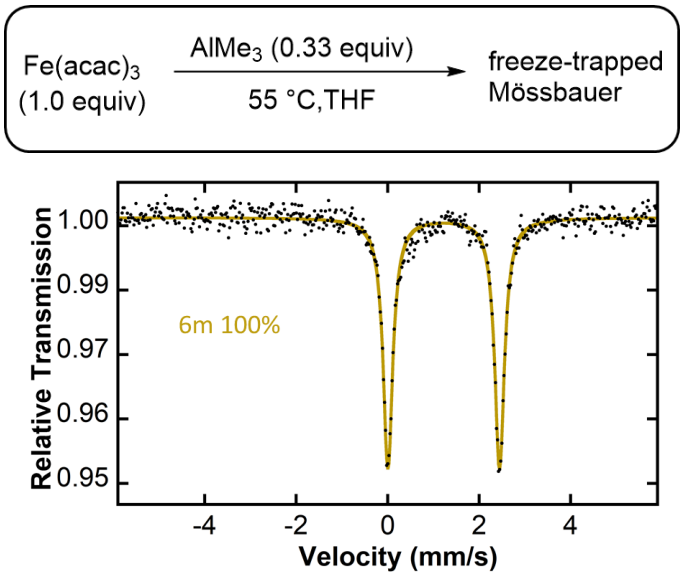

Figure S10. 80 K ^{57}Fe Mössbauer spectrum of a freeze-trapped solution following the reaction of $Fe(acac)_3$ (1.0 equiv) with $AlMe_3$ (0.33 equiv). Data (black dots) and fit components are shown. Yellow component has parameters δ = 1.23 mm/s and $|\Delta E_Q|$ = 2.45 mm/s. These parameters are consistent with the reduction of $Fe(acac)_3$ to a high-spin iron(II) complex.

3. X-ray Crystallographic Data

3.1 CCDC Deposition. The reported crystal structure has been deposited with the Cambridge Crystallographic Data Center (CCDC). The crystal structure was assigned the following CCDC deposition number:

$Fe(dppen)_2(Me)_2$: 2111349

3.2 $Fe(dppen)_2(Me)_2$

REFERENCE NUMBER: neijd07

CRYSTAL STRUCTURE REPORT

$C_{54}\ H_{50}\ Fe\ P_4$

or

$Fe(dppen)_2(Me)_2 \cdot xSolvent$

Report prepared for:

J. DeMuth, Prof. M. Neidig

August 23, 2021

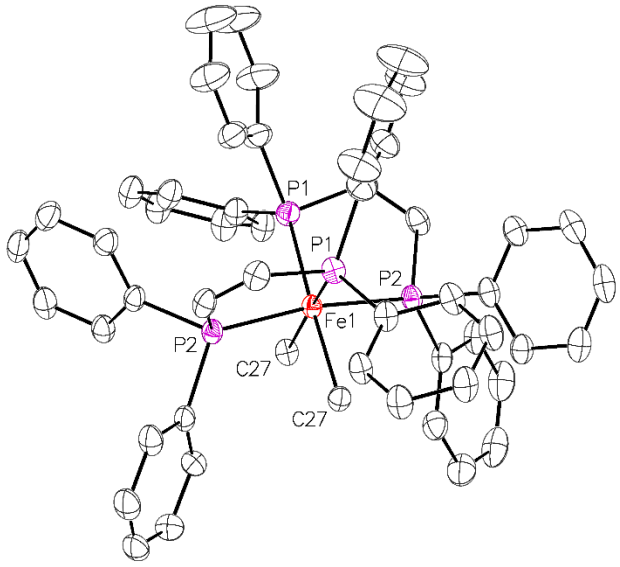

William W. Brennessel

X-ray Crystallographic Facility

Department of Chemistry, University of Rochester

120 Trustee Road

Rochester, NY 14627

Data collection

A crystal (0.295 x 0.215 x 0.104 mm^3) was placed onto a thin glass optical fiber or a nylon loop and mounted on a Rigaku XtaLAB Synergy-S Dualflex diffractometer equipped with a HyPix-6000HE HPC area detector for data collection at 100.00(10) K. A preliminary set of cell constants and an orientation matrix were calculated from a small sampling of reflections.[1] A short pre-experiment was run, from which an optimal data collection strategy was determined. The full data collection was carried out using a PhotonJet (Cu) X-ray source with frame times of 0.71 and 2.86 seconds and a detector distance of 34.0 mm. Series of frames were collected in 0.50º steps in ω at different 2θ, κ, and ϕ settings. After the intensity data were corrected for absorption, the final cell constants were calculated from the xyz centroids of 24188 strong reflections from the actual data collection after integration.[1] See Table 1 for additional crystal and refinement information.

Structure solution and refinement

The structure was solved using SHELXT[2] and refined using SHELXL.[3] The space group *C*2/*c* was determined based on systematic absences and intensity statistics. Most or all non-hydrogen atoms were assigned from the solution. Full-matrix least squares / difference Fourier cycles were performed which located any remaining non-hydrogen atoms. All non-hydrogen atoms were refined with anisotropic displacement parameters. The methyl ligand's hydrogen atoms were found from the difference Fourier map and refined freely. All other hydrogen atoms were placed in ideal positions and refined as riding atoms with relative isotropic displacement parameters.

Reflection contributions from highly disordered solvent were fixed and added the calculated structures using the SQUEEZE routine of program Platon,[4] which determined there to be 520 electrons in 1965 $Å^3$ per unit cell treated this way. Because the exact identity and amount of solvent were unknown, no solvent was included in the atom list or molecular formula. Thus all calculated quantities that derive from the molecular formula (e.g., F(000), density, molecular weight, etc.) are known to be inaccurate.

The final full matrix least squares refinement converged to $R1 = 0.0464$ (F^2, $I > 2\sigma(I)$) and $wR2 = 0.1262$ (F^2, all data).

Structure description

The structure is the one suggested. The asymmetric unit contains one-half of an iron molecule on a crystallographic two-fold axis that includes the metal center and highly disordered solvent molecules whose individual atoms were not assigned (see above).

Structure manipulation and figure generation were performed using Olex2.[5] Unless noted otherwise all structural diagrams containing anisotropic displacement ellipsoids are drawn at the 50 % probability level.

Data collection, structure solution, and structure refinement were conducted at the X-ray Crystallographic Facility, B04 Hutchison Hall, Department of Chemistry, University of Rochester. The instrument was purchased with funding from NSF MRI program grant CHE-1725028. All publications arising from this report MUST either 1) include William W. Brennessel as a coauthor or 2) acknowledge William W. Brennessel and the X-ray Crystallographic Facility of the Department of Chemistry at the University of Rochester.

---

[1] *CrysAlisPro*, version 171.41.112a; Rigaku Corporation: Oxford, UK, 2021.

[2] Sheldrick, G. M. *SHELXT*, version 2018/2; *Acta. Crystallogr.* **2015**, *A71*, 3-8.

[3] Sheldrick, G. M. *SHELXL*, version 2018/3; *Acta. Crystallogr.* **2015**, *C71*, 3-8.

[4] Spek, A. L. *PLATON*, version 250420; *Acta. Crystallogr.* **2015**, *C71*, 9-18.

[5] Dolomanov, O. V.; Bourhis, L. J.; Gildea, R. J.; Howard, J. A. K.; Puschmann, H. *Olex2*, version 1.3-ac4; *J. Appl. Cryst.* **2009**, *42*, 339-341.

Some equations of interest:

$$R_{int} = \Sigma\, |F_o^2 - < F_o^2 >| \,/\, \Sigma |F_o^2|$$

$$R1 = \Sigma ||F_o| - |F_c|| \,/\, \Sigma |F_o|$$

$$wR2 = [\Sigma [w(F_o^2 - F_c^2)^2] \,/\, \Sigma\, [w(F_o^2)^2]]^{1/2}$$

where $w = 1 \,/\, [\sigma^2 (F_o^2) + (aP)^2 + bP]$ and

$$P = 1/3 \max (0, F_o^2) + 2/3\, F_c^2$$

$$\text{GOF} = S = [\Sigma [w(F_o^2 - F_c^2)^2] \,/\, (m-n)]^{1/2}$$

where m = number of reflections and n = number of parameters

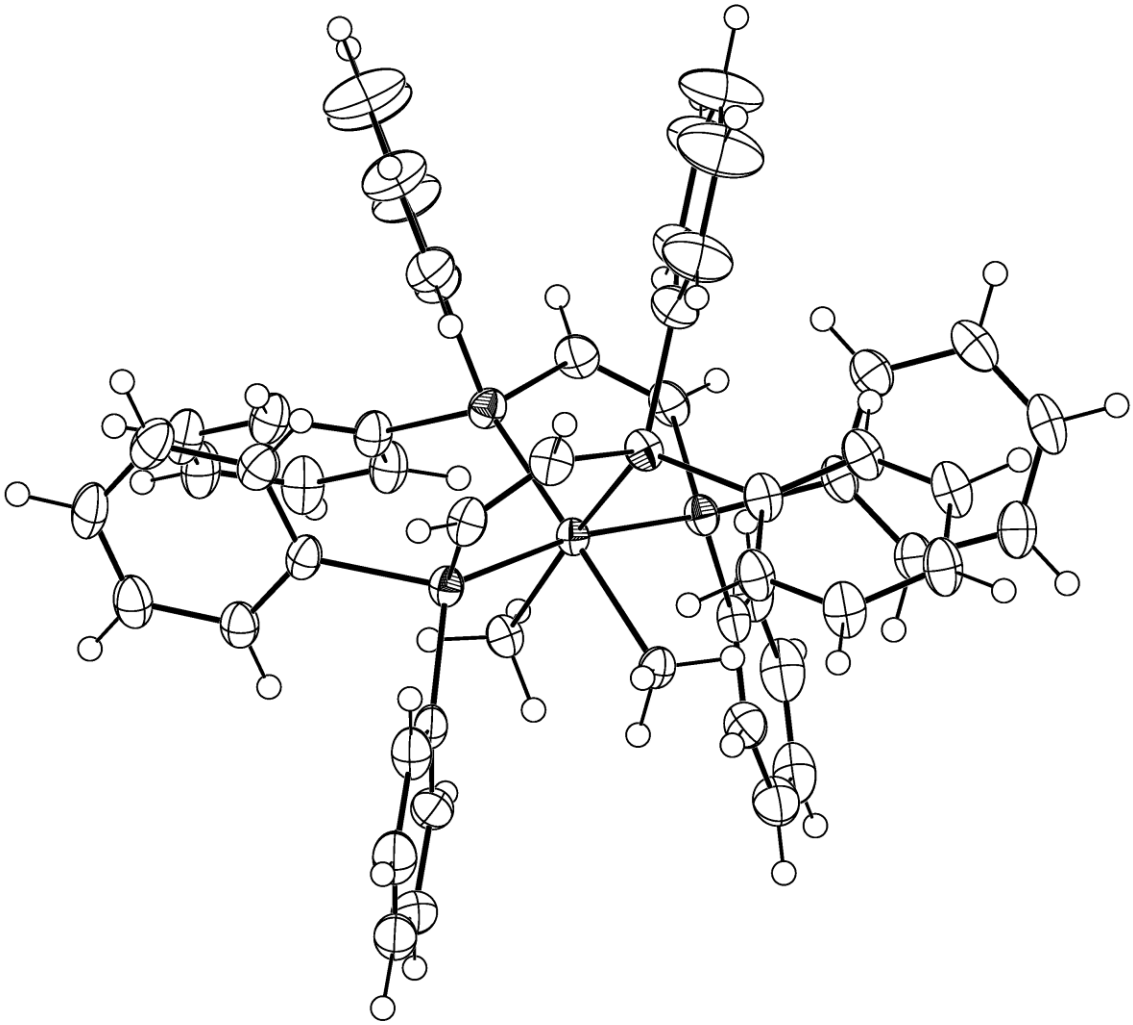

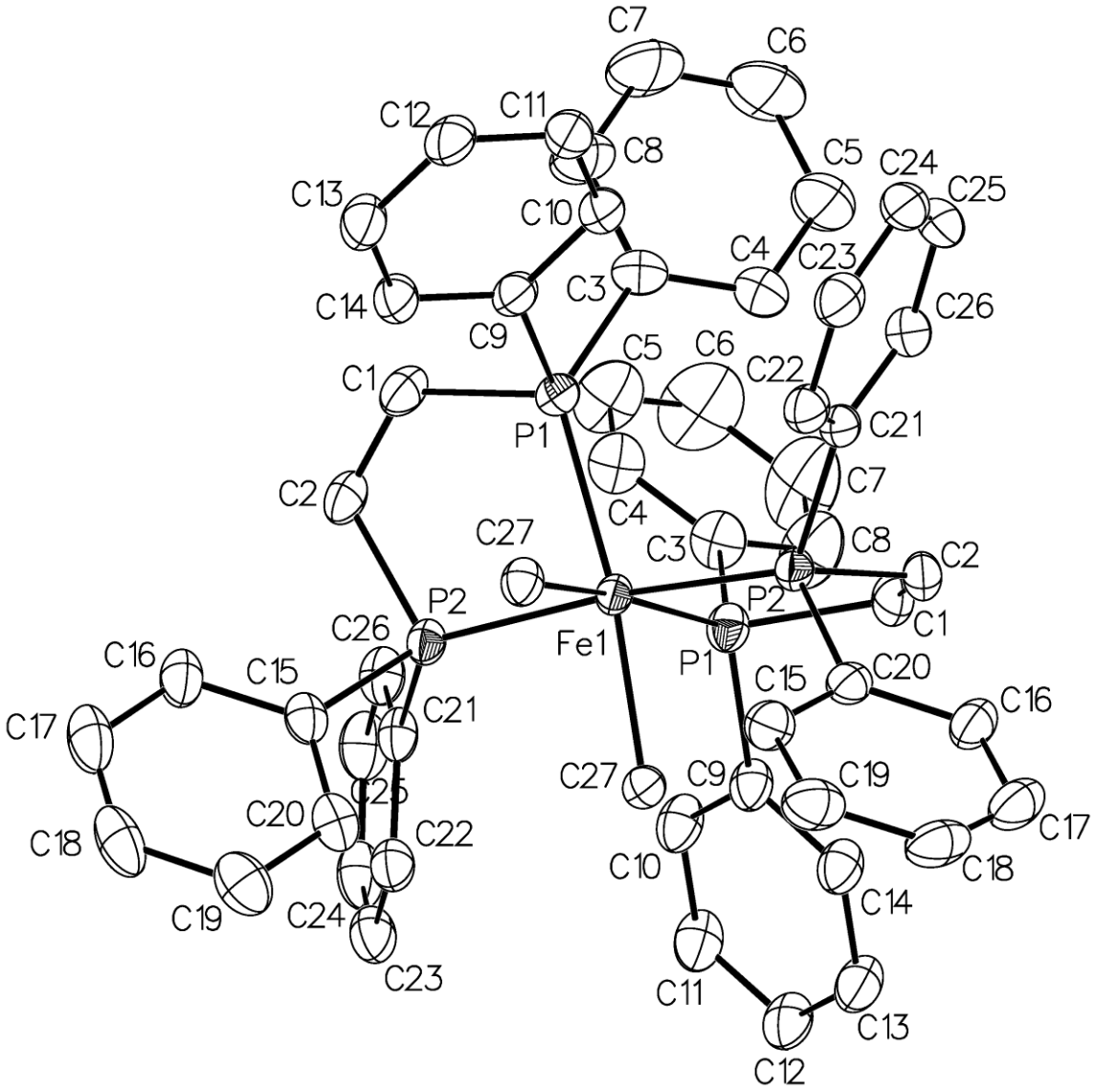
C7
C6
C12
C11
C8
C5
C24
C25
C13
C10
C4
C23
C14
C3
C26
C9
C5
C6
C22
C1
P1
C21
C2
C7
C4
C27
C3
C8
C2
P2
P2
C1
C26
Fe1
P1
C16
C15
C15
C20
C16
C17
C21
C27
C9
C19
C17
C25
C20
C22
C18
C10
C18
C14
C19
C24
C23
C11
C13
C12

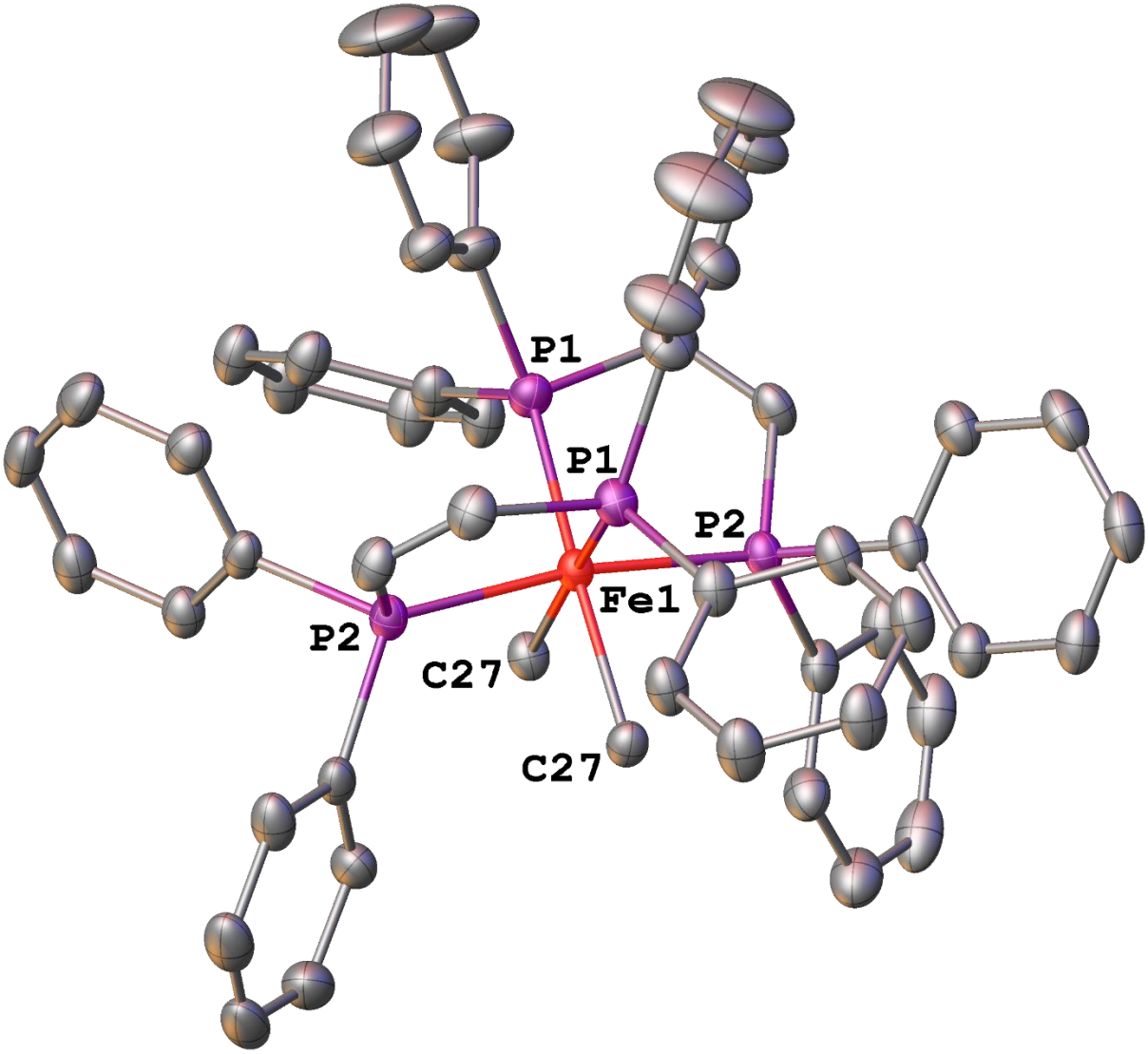
P1
P1
P2
Fe1
P2
C27
C27

Table 1. Crystal data and structure refinement for neijd07.

Identification code	neijd07	
Empirical formula	C54 H50 Fe P4	
Formula weight	878.67	
Temperature	100.00(10) K	
Wavelength	1.54184 Å	
Crystal system	monoclinic	
Space group	*C*2/*c*	
Unit cell dimensions	a = 11.40452(13) Å	α = 90°
	b = 26.0935(3) Å	β = 96.6965(10)°
	c = 19.63981(19) Å	γ = 90°
Volume	5804.62(11) Å^3	
Z	4	
Density (calculated)	1.005 Mg/m^3	
Absorption coefficient	3.336 mm^{-1}	
F(000)	1840	
Crystal color, morphology	red, block	
Crystal size	0.295 x 0.215 x 0.104 mm^3	
Theta range for data collection	3.388 to 80.310°	
Index ranges	$-14 \le h \le 14$, $-32 \le k \le 33$, $-25 \le l \le 23$	
Reflections collected	48565	
Independent reflections	6239 [R(int) = 0.0761]	
Observed reflections	5773	
Completeness to theta = 74.504°	99.8%	
Absorption correction	Multi-scan	
Max. and min. transmission	1.00000 and 0.49271	
Refinement method	Full-matrix least-squares on F^2	
Data / restraints / parameters	6239 / 0 / 279	
Goodness-of-fit on F^2	1.050	
Final R indices [I>2sigma(I)]	R1 = 0.0464, wR2 = 0.1243	
R indices (all data)	R1 = 0.0491, wR2 = 0.1262	
Largest diff. peak and hole	0.900 and -0.449 e.Å^{-3}	

Table 2. Atomic coordinates (x 10^4) and equivalent isotropic displacement parameters ($Å^2$x 10^3) for neijd07. U_{eq} is defined as one third of the trace of the orthogonalized U_{ij} tensor.

	x	y	z	U_{eq}
Fe1	5000	6871(1)	2500	19(1)
P1	3501(1)	6336(1)	2195(1)	25(1)
P2	4284(1)	6941(1)	3498(1)	22(1)
C1	2714(2)	6236(1)	2950(1)	30(1)
C2	3038(2)	6502(1)	3511(1)	28(1)
C3	3607(2)	5667(1)	1899(1)	34(1)
C4	4657(2)	5484(1)	1698(1)	36(1)
C5	4751(3)	4983(1)	1479(2)	53(1)
C6	3800(3)	4660(1)	1454(2)	75(1)
C7	2738(3)	4837(1)	1645(2)	76(1)
C8	2643(2)	5335(1)	1865(2)	54(1)
C9	2187(2)	6518(1)	1594(1)	28(1)
C10	2097(2)	6374(1)	905(1)	32(1)
C11	1104(2)	6505(1)	459(1)	36(1)
C12	193(2)	6780(1)	691(1)	36(1)
C13	273(2)	6924(1)	1372(1)	37(1)
C14	1265(2)	6794(1)	1820(1)	32(1)
C15	3630(2)	7549(1)	3766(1)	26(1)
C16	2576(2)	7551(1)	4067(1)	34(1)
C17	2115(2)	8002(1)	4300(1)	42(1)
C18	2694(2)	8455(1)	4247(1)	44(1)
C19	3747(2)	8466(1)	3951(1)	40(1)
C20	4206(2)	8017(1)	3710(1)	32(1)
C21	5112(2)	6779(1)	4337(1)	26(1)
C22	5837(2)	7141(1)	4702(1)	29(1)
C23	6470(2)	7016(1)	5328(1)	35(1)
C24	6402(2)	6527(1)	5592(1)	38(1)
C25	5674(2)	6166(1)	5241(1)	38(1)
C26	5029(2)	6291(1)	4618(1)	32(1)
C27	6242(2)	7445(1)	2830(1)	25(1)

Table 3. Bond lengths [Å] and angles [°] for neijd07.

Fe(1)-P(1)#1	2.2338(5)	C(13)-H(13)	0.9500
Fe(1)-P(1)	2.2338(5)	C(13)-C(14)	1.392(3)
Fe(1)-P(2)	2.2163(4)	C(14)-H(14)	0.9500
Fe(1)-P(2)#1	2.2163(4)	C(15)-C(16)	1.400(3)
Fe(1)-C(27)	2.1093(19)	C(15)-C(20)	1.396(3)
Fe(1)-C(27)#1	2.1092(19)	C(16)-H(16)	0.9500
P(1)-C(1)	1.840(2)	C(16)-C(17)	1.388(3)
P(1)-C(3)	1.849(2)	C(17)-H(17)	0.9500
P(1)-C(9)	1.858(2)	C(17)-C(18)	1.364(4)
P(2)-C(2)	1.828(2)	C(18)-H(18)	0.9500
P(2)-C(15)	1.855(2)	C(18)-C(19)	1.394(4)
P(2)-C(21)	1.8510(19)	C(19)-H(19)	0.9500
C(1)-H(1)	0.9500	C(19)-C(20)	1.387(3)
C(1)-C(2)	1.319(3)	C(20)-H(20)	0.9500
C(2)-H(2)	0.9500	C(21)-C(22)	1.397(3)
C(3)-C(4)	1.389(3)	C(21)-C(26)	1.396(3)
C(3)-C(8)	1.395(3)	C(22)-H(22)	0.9500
C(4)-H(4)	0.9500	C(22)-C(23)	1.390(3)
C(4)-C(5)	1.384(3)	C(23)-H(23)	0.9500
C(5)-H(5)	0.9500	C(23)-C(24)	1.383(3)
C(5)-C(6)	1.370(4)	C(24)-H(24)	0.9500
C(6)-H(6)	0.9500	C(24)-C(25)	1.385(4)
C(6)-C(7)	1.388(5)	C(25)-H(25)	0.9500
C(7)-H(7)	0.9500	C(25)-C(26)	1.391(3)
C(7)-C(8)	1.378(4)	C(26)-H(26)	0.9500
C(8)-H(8)	0.9500	C(27)-H(27A)	1.00(2)
C(9)-C(10)	1.398(3)	C(27)-H(27B)	0.96(2)
C(9)-C(14)	1.389(3)	C(27)-H(27C)	0.95(3)
C(10)-H(10)	0.9500	P(1)-Fe(1)-P(1)#1	102.65(3)
C(10)-C(11)	1.392(3)	P(2)-Fe(1)-P(1)#1	99.405(18)
C(11)-H(11)	0.9500	P(2)-Fe(1)-P(1)	86.531(18)
C(11)-C(12)	1.383(3)	P(2)#1-Fe(1)-P(1)	99.405(18)
C(12)-H(12)	0.9500	P(2)#1-Fe(1)-P(1)#1	86.530(18)
C(12)-C(13)	1.382(3)	P(2)-Fe(1)-P(2)#1	170.56(3)

C(27)-Fe(1)-P(1)	172.25(6)	C(5)-C(6)-H(6)	120.1
C(27)-Fe(1)-P(1)#1	84.00(6)	C(5)-C(6)-C(7)	119.9(3)
C(27)#1-Fe(1)-P(1)	84.00(6)	C(7)-C(6)-H(6)	120.1
C(27)#1-Fe(1)-P(1)#1	172.26(6)	C(6)-C(7)-H(7)	120.0
C(27)-Fe(1)-P(2)	88.47(5)	C(8)-C(7)-C(6)	120.1(3)
C(27)-Fe(1)-P(2)#1	84.83(5)	C(8)-C(7)-H(7)	120.0
C(27)#1-Fe(1)-P(2)	84.83(5)	C(3)-C(8)-H(8)	119.7
C(27)#1-Fe(1)-P(2)#1	88.47(5)	C(7)-C(8)-C(3)	120.7(3)
C(27)#1-Fe(1)-C(27)	89.66(11)	C(7)-C(8)-H(8)	119.7
C(1)-P(1)-Fe(1)	107.63(7)	C(10)-C(9)-P(1)	120.60(15)
C(1)-P(1)-C(3)	100.04(10)	C(14)-C(9)-P(1)	120.95(15)
C(1)-P(1)-C(9)	96.56(9)	C(14)-C(9)-C(10)	118.45(18)
C(3)-P(1)-Fe(1)	126.79(7)	C(9)-C(10)-H(10)	119.8
C(3)-P(1)-C(9)	96.79(10)	C(11)-C(10)-C(9)	120.39(19)
C(9)-P(1)-Fe(1)	123.16(7)	C(11)-C(10)-H(10)	119.8
C(2)-P(2)-Fe(1)	109.16(7)	C(10)-C(11)-H(11)	119.7
C(2)-P(2)-C(15)	101.11(9)	C(12)-C(11)-C(10)	120.51(19)
C(2)-P(2)-C(21)	99.27(9)	C(12)-C(11)-H(11)	119.7
C(15)-P(2)-Fe(1)	121.54(6)	C(11)-C(12)-H(12)	120.2
C(21)-P(2)-Fe(1)	124.49(6)	C(13)-C(12)-C(11)	119.5(2)
C(21)-P(2)-C(15)	97.05(8)	C(13)-C(12)-H(12)	120.2
P(1)-C(1)-H(1)	120.6	C(12)-C(13)-H(13)	119.9
C(2)-C(1)-P(1)	118.86(15)	C(12)-C(13)-C(14)	120.2(2)
C(2)-C(1)-H(1)	120.6	C(14)-C(13)-H(13)	119.9
P(2)-C(2)-H(2)	121.3	C(9)-C(14)-C(13)	120.93(19)
C(1)-C(2)-P(2)	117.46(15)	C(9)-C(14)-H(14)	119.5
C(1)-C(2)-H(2)	121.3	C(13)-C(14)-H(14)	119.5
C(4)-C(3)-P(1)	120.27(16)	C(16)-C(15)-P(2)	121.10(17)
C(4)-C(3)-C(8)	118.3(2)	C(20)-C(15)-P(2)	121.14(15)
C(8)-C(3)-P(1)	121.46(19)	C(20)-C(15)-C(16)	117.66(19)
C(3)-C(4)-H(4)	119.5	C(15)-C(16)-H(16)	119.4
C(5)-C(4)-C(3)	120.9(2)	C(17)-C(16)-C(15)	121.3(2)
C(5)-C(4)-H(4)	119.5	C(17)-C(16)-H(16)	119.4
C(4)-C(5)-H(5)	119.9	C(16)-C(17)-H(17)	119.9
C(6)-C(5)-C(4)	120.2(3)	C(18)-C(17)-C(16)	120.3(2)
C(6)-C(5)-H(5)	119.9	C(18)-C(17)-H(17)	119.9

C(17)-C(18)-H(18)	120.1	C(24)-C(23)-H(23)	119.9
C(17)-C(18)-C(19)	119.8(2)	C(23)-C(24)-H(24)	120.1
C(19)-C(18)-H(18)	120.1	C(23)-C(24)-C(25)	119.9(2)
C(18)-C(19)-H(19)	119.9	C(25)-C(24)-H(24)	120.1
C(20)-C(19)-C(18)	120.2(2)	C(24)-C(25)-H(25)	119.9
C(20)-C(19)-H(19)	119.9	C(24)-C(25)-C(26)	120.1(2)
C(15)-C(20)-H(20)	119.6	C(26)-C(25)-H(25)	119.9
C(19)-C(20)-C(15)	120.8(2)	C(21)-C(26)-H(26)	119.7
C(19)-C(20)-H(20)	119.6	C(25)-C(26)-C(21)	120.6(2)
C(22)-C(21)-P(2)	120.81(15)	C(25)-C(26)-H(26)	119.7
C(26)-C(21)-P(2)	120.65(16)	Fe(1)-C(27)-H(27A)	112.0(14)
C(26)-C(21)-C(22)	118.54(18)	Fe(1)-C(27)-H(27B)	111.8(14)
C(21)-C(22)-H(22)	119.7	Fe(1)-C(27)-H(27C)	111.7(15)
C(23)-C(22)-C(21)	120.6(2)	H(27A)-C(27)-H(27B)	108.2(19)
C(23)-C(22)-H(22)	119.7	H(27A)-C(27)-H(27C)	107(2)
C(22)-C(23)-H(23)	119.9	H(27B)-C(27)-H(27C)	106(2)
C(24)-C(23)-C(22)	120.2(2)		

Symmetry transformations used to generate equivalent atoms:

#1 -x+1,y,-z+1/2

Table 4. Anisotropic displacement parameters ($Å^2 x\ 10^3$) for neijd07. The anisotropic displacement factor exponent takes the form: $-2\pi^2[\ h^2\ a^{*2}U_{11} + ... + 2\ h\ k\ a^*\ b^*\ U_{12}\ ]$

	U_{11}	U_{22}	U_{33}	U_{23}	U_{13}	U_{12}
Fe1	16(1)	24(1)	17(1)	0	3(1)	0
P1	21(1)	28(1)	24(1)	-2(1)	3(1)	-4(1)
P2	19(1)	28(1)	19(1)	1(1)	4(1)	1(1)
C1	23(1)	36(1)	32(1)	4(1)	6(1)	-6(1)
C2	22(1)	38(1)	25(1)	7(1)	7(1)	-1(1)
C3	35(1)	29(1)	38(1)	-6(1)	3(1)	-7(1)
C4	40(1)	32(1)	38(1)	-8(1)	6(1)	-4(1)
C5	52(2)	37(1)	70(2)	-18(1)	12(1)	-2(1)
C6	77(2)	35(1)	116(3)	-30(2)	18(2)	-10(1)
C7	63(2)	46(2)	121(3)	-25(2)	23(2)	-26(2)
C8	42(1)	40(1)	81(2)	-16(1)	13(1)	-14(1)
C9	21(1)	38(1)	25(1)	-1(1)	2(1)	-5(1)
C10	24(1)	44(1)	28(1)	-8(1)	4(1)	-4(1)
C11	29(1)	53(1)	26(1)	-7(1)	4(1)	-6(1)
C12	23(1)	58(1)	28(1)	-2(1)	-1(1)	-4(1)
C13	24(1)	57(2)	30(1)	-3(1)	4(1)	2(1)
C14	25(1)	46(1)	24(1)	-4(1)	4(1)	-1(1)
C15	25(1)	35(1)	18(1)	1(1)	1(1)	7(1)
C16	25(1)	51(1)	26(1)	-1(1)	4(1)	8(1)
C17	34(1)	60(2)	31(1)	-3(1)	5(1)	20(1)
C18	48(1)	53(2)	30(1)	-6(1)	2(1)	28(1)
C19	49(1)	36(1)	35(1)	-1(1)	3(1)	12(1)
C20	36(1)	32(1)	28(1)	-1(1)	8(1)	7(1)
C21	23(1)	36(1)	20(1)	4(1)	5(1)	7(1)
C22	26(1)	38(1)	24(1)	0(1)	4(1)	3(1)
C23	30(1)	52(1)	24(1)	-3(1)	4(1)	5(1)
C24	35(1)	58(2)	21(1)	8(1)	6(1)	13(1)
C25	41(1)	44(1)	30(1)	13(1)	11(1)	10(1)
C26	31(1)	37(1)	28(1)	5(1)	8(1)	4(1)
C27	22(1)	30(1)	22(1)	-2(1)	3(1)	-3(1)

Table 5. Hydrogen coordinates (x 10^4) and isotropic displacement parameters ($Å^2$ x 10^3) for neijd07.

	x	y	z	U(eq)
H1	2085	5996	2936	36
H2	2638	6468	3907	34
H4	5320	5706	1710	44
H5	5477	4862	1347	64
H6	3867	4316	1306	90
H7	2075	4614	1623	91
H8	1914	5453	1996	65
H10	2718	6185	740	38
H11	1051	6405	-9	43
H12	-482	6870	384	44
H13	-351	7113	1535	44
H14	1312	6896	2287	38
H16	2168	7238	4113	41
H17	1392	7996	4496	50
H18	2382	8763	4412	52
H19	4151	8781	3913	48
H20	4920	8028	3506	38
H22	5898	7477	4521	35
H23	6952	7266	5575	43
H24	6852	6439	6013	46
H25	5616	5831	5426	45
H26	4528	6042	4382	38
H27A	5930(20)	7795(9)	2714(12)	29(6)
H27B	6470(20)	7429(9)	3317(12)	27(6)
H27C	6950(20)	7408(9)	2622(12)	31(6)

Table 6. Torsion angles [°] for neijd07.

Fe1-P1-C1-C2	5.40(19)	C6-C7-C8-C3	0.1(6)
Fe1-P1-C3-C4	-14.8(2)	C8-C3-C4-C5	-0.9(4)
Fe1-P1-C3-C8	165.75(19)	C9-P1-C1-C2	-122.50(18)
Fe1-P1-C9-C10	99.31(18)	C9-P1-C3-C4	126.19(19)
Fe1-P1-C9-C14	-81.37(18)	C9-P1-C3-C8	-53.3(2)
Fe1-P2-C2-C1	-2.83(19)	C9-C10-C11-C12	0.1(4)
Fe1-P2-C15-C16	136.16(14)	C10-C9-C14-C13	0.1(3)
Fe1-P2-C15-C20	-47.52(18)	C10-C11-C12-C13	-0.1(4)
Fe1-P2-C21-C22	86.92(17)	C11-C12-C13-C14	0.2(4)
Fe1-P2-C21-C26	-92.80(16)	C12-C13-C14-C9	-0.2(4)
P1-C1-C2-P2	-1.7(2)	C14-C9-C10-C11	-0.1(3)
P1-C3-C4-C5	179.6(2)	C15-P2-C2-C1	126.41(17)
P1-C3-C8-C7	-179.9(3)	C15-P2-C21-C22	-49.51(17)
P1-C9-C10-C11	179.23(17)	C15-P2-C21-C26	130.77(16)
P1-C9-C14-C13	-179.19(18)	C15-C16-C17-C18	-0.9(3)
P2-C15-C16-C17	176.74(16)	C16-C15-C20-C19	0.4(3)
P2-C15-C20-C19	-176.03(16)	C16-C17-C18-C19	0.8(3)
P2-C21-C22-C23	-179.09(15)	C17-C18-C19-C20	-0.1(3)
P2-C21-C26-C25	178.42(16)	C18-C19-C20-C15	-0.5(3)
C1-P1-C3-C4	-135.88(19)	C20-C15-C16-C17	0.3(3)
C1-P1-C3-C8	44.7(2)	C21-P2-C2-C1	-134.45(17)
C1-P1-C9-C10	-144.63(18)	C21-P2-C15-C16	-85.63(17)
C1-P1-C9-C14	34.69(19)	C21-P2-C15-C20	90.68(17)
C2-P2-C15-C16	15.30(17)	C21-C22-C23-C24	0.9(3)
C2-P2-C15-C20	-168.38(16)	C22-C21-C26-C25	-1.3(3)
C2-P2-C21-C22	-152.04(16)	C22-C23-C24-C25	-1.8(3)
C2-P2-C21-C26	28.24(18)	C23-C24-C25-C26	1.1(3)
C3-P1-C1-C2	139.38(18)	C24-C25-C26-C21	0.4(3)
C3-P1-C9-C10	-43.65(19)	C26-C21-C22-C23	0.6(3)
C3-P1-C9-C14	135.67(19)		
C3-C4-C5-C6	0.5(5)		
C4-C3-C8-C7	0.6(5)		
C4-C5-C6-C7	0.3(6)		
C5-C6-C7-C8	-0.6(6)		

Symmetry transformations used to generate equivalent atoms: #1 -x+1,y,-z+1/2

References

1. R. Shang, L. Ilies, S. Asako and E. Nakamura, *Journal of the American Chemical Society*, 2014, **136**, 14349-14352.
2. R. Shang, L. Ilies and E. Nakamura, *Journal of the American Chemical Society*, 2015, **137**, 7660-7663.
3. M. G. T. C. Ribeiro and A. A. S. C. Machado, *Journal of Chemical Education*, 2011, **88**, 947-953.